I

HEAT TRANSFER AND PRESSURE DROP MEASUREMENTS FOR HIGH TEMPERATURE BOILING POTASSIUM IN FORCED CONVECTION

J.A. Bond
J.R. Peterson
F.E. Tippets

INTRODUCTION

An investigation of boiling and condensing potassium heat transfer is being conducted for the National Aeronautics and Space Administration by General Electric Company under Contract NAS 3-2528 to obtain two-phase heat transfer and fluid flow data for potassium under conditions of boiling and condensing at temperatures anticipated in turbo-electric Rankine cycle systems. The purpose of this paper is to present some of the results obtained from the boiling studies done under this program.

Experimental work with boiling potassium includes both "once-through" two-fluid boiler tests in Haynes-25 alloy facility with single-tube geometries at potassium temperatures to 1750^{o}F, and complementary boiling experiments with a radiant-heated Cb-1Zr facility at potassium temperatures to 2100^{o}F. Results from these experiments include measurements of heat transfer coefficients in the various boiling regimes from low vapor quality to superheated vapor conditions, two-phase pressure drop measurements, and some exploratory critical heat flux determinations.

EXPERIMENTAL APPARATUS AND INSTRUMENTATION

300 KW Two-Fluid Facility

The 300 KW two-fluid liquid metal test facility (Figure 1) is constructed of Haynes-25 alloy. Liquid sodium flows in the primary loop of the facility, accepting heat from a gas fired furnace at maximum sodium temperatures to 1850^{o}F and rejecting the heat at the test section to boiling potassium in the secondary loop. Potassium flowing in the secondary loop is condensed in vertical and horizontal air-cooled single-tube condensers. The potassium vapor-liquid interface is maintained in a head tank fitted with level probes, positioned immediately downstream of the horizontal condenser. Flow rates are measured by electromagnetic flowmeters in the primary and secondary loops. Control of oxygen concentration in both loops is accomplished by zirconium gettering grids located in the dump tanks.

Figure 2 shows a disassembled view of the boiling test section, including one of the helical inserts employed. The test section is a shell and tube heat exchanger with the potassium flowing inside the boiler tube and heated by sodium flowing in the annulus. Relative expansion between the boiler tube and the shell is accommodated by a bellows located before the heated section of the tube near the potassium inlet. The helix insert consists of a 1/4-inch outside diameter support tube around which is wound a ribbon to form a helical flow path when the insert is placed in the boiler tube.

Seven 1/16-inch diameter Inconel sheathed chromel-alumel thermocouples are located in the insert support tube, entering from the outlet end, to measure potassium temperature distribution. Thermocouple wells, each containing three calibrated platinum-platinum 10% rhodium Haynes-25 alloy sheathed thermocouples, are located at the test section inlet and exit of both the sodium and the potassium streams. Inconel sheathed platinum-platinum 10% rhodium thermocouples are positioned on the outside shell of the test section in eleven rings of five thermocouples each to measure the sodium axial temperature distribution (Figure 3).

All the thermocouples in the inlet and exit wells were calibrated periodically in a melting point apparatus and were used as primary standards for the in-loop calibration of the shell and insert thermocouples. Calibration of the shell thermocouples and determination of test section heat losses were done by maintaining the primary loop at temperature with the secondary loop evacuated, under which conditions the temperature change between the sodium inlet and exit wells is due solely to heat loss. The heat loss determinations were made at a very low sodium flow rate in order to maximize the sodium temperature change across the test section. The shell thermocouples were calibrated relative to the primary side well thermocouples at near-isothermal conditions attained by use of the maximum sodium flow rate. The insert thermocouples were calibrated against the potassium exit well thermocouples under boiling conditions at low flow and low vapor quality, for which the temperature changes along the insert and between the insert end and the outlet well were negligible.

The thermocouple calibrations were performed at various temperature levels and the corrections obtained were then applied as functions of sodium and potassium temperatures at the test section, respectively, in the data reduction procedure. The test section heat loss, which was of the order of 1 KW was also determined as a function of sodium temperature. The thermocouple corrections were generally less than $10^{o}F$, and no appreciable drift was detected over the course of the experiments. The temperature measurements are believed to be accurate to within $\pm$ $2^{o}F$ with the procedures followed.

The relationship between flow rate and output signal from the electromagnetic flowmeters in both loops of the facility were obtained by calculation using the equations given in Reference 1. In order to minimize errors, measured values of the field intensity of the magnets were used for the calculations. An indication of the resulting accuracy in flow determination was obtained through intercalibration of the two flowmeters by heat balance around the test section, using liquid-

liquid runs. The disagreement obtained was 2%, which is believed to be representative of the probable error in the individual loop flow rate determinations.

The two-phase potassium pressure loss in the test section was determined by means of two slack-diaphragm pressure transducers, with pressure taps positioned at the potassium inlet and exit (Figure 1). These pressure gages were calibrated against a Wallace and Tiernan (type FA-145) standard gage by filling the potassium loop to various pressures with argon both before and after the experiments with each test section. The calibrations before and after testing generally agreed to within 1-psi; thus the error of the pressure measurements is taken to be less than 1-psi. This accuracy was attained by maintaining the diaphragm of the transducers at a constant temperature level, which was necessary since the gage calibration depends on the diaphragm temperature.

Measurements of potassium exit pressure together with exit temperature were used as one means to determine the amount of vapor superheat in the once-through boiling tests in the 300 KW Facility. Figure 4 shows the measured potassium exit pressure plotted against the measured exit temperature for several runs in which superheated vapor exit conditions were attained. Also plotted are data for which the calculated exit vapor quality was between 10% and 90%. The latter results agree generally, within 1-psi, with the saturation curve as determined by the Naval Research Laboratories (Reference 10). This is a further indication of the accuracy of the pressure measurements.

Recording of the large number of instrument readings required to define a single data point in the 300 KW Facility is accomplished through the use of a high speed digital recorder.

Complete readout on paper tape of the approximately 150 information bits required is obtained in approximately one minute. Three complete readouts were obtained for each data point, in order to provide an indication of the presence or absence of significant fluctuations.

100 KW High Temperature Facility

The 100 KW Facility is a single loop system used to study heat transfer to boiling potassium at fluid temperatures up to 2100°F. The alkali metal containment piping is constructed from columbium-1% zirconium and is enclosed in a high-vacuum environmental chamber to avoid atmospheric contamination. Figure 5 is a schematic representation of the loop and principal instrumentation.

Liquid potassium is discharged from the electromagnetic pump and flows through an electromagnetic flowmeter to an 8 KW radiant preheater, which controls the preboiler inlet subcooling. Upon leaving the preheater the potassium flows through a throttling orifice into the preboiler, and then, in vertical up-flow, into the test section.

The preboiler consists of a helically wound section of pipe with a radiant heater element in the core of the helix, all contained in a radiation shield (Figure 6). The preboiler heater element is fabricated from coiled tungsten wire and is operated at gross electrical power levels up to 60 KW. The function of the preboiler is to control the enthalpy of the potassium in the test section independent of test section heat flux, thus permitting separation of the effects of quality and heat flux in the tests.

The test section, located downstream of the preboiler, is a vertical section of pipe with a 30-inch heated length. The radiant heater for the test section consists of an array of 27 tungsten rods surrounding the test section, together with a radiation shield (Figure 7). The test section heater is operated at gross electrical power levels up to 32 KW.

Heat is rejected from the system in approximately 60 ft. of condenser piping radiating to the water-cooled walls of the environmental chamber. Some control of the heat rejection rate is accomplished with adjustable shutters which surround the condenser coil (Figure 7).

The preboiler and the test section radiation shields consist of concentric tantalum sheets enclosed in stainless steel cases. The temperature of each of these cases is measured at six locations and these temperatures are used to determine heat losses using heat loss calibration data. The heat loss calibrations are performed with the preboiler and test section piping removed. With the vacuum chamber evacuated, power is supplied to the heaters and the corresponding steady-state radiation shield case temperatures are measured. This procedure is repeated at several power levels, and since all the power supplied is lost through the shield a direct correlation of heat loss as a function of shield case temperature is obtained.

The principal measurements and corresponding instrumentation are as follows:

a) The flow rate is measured with an electromagnetic flowmeter. Calibration of the flowmeter is by the calorimetric method using an energy balance across the test section with all liquid flow. The range of error of the flow rate measurements is estimated to be within ± 10%, depending on the accuracy of the potassium liquid specific heat data used (Reference 10), which was assumed for this flow rate error estimation to be within ± 5%.

b) Power to the preboiler and test section is measured with polyphase wattmeters. The estimated range of error of the electrical power measurements is ± 1%.

c) Fluid temperatures at the preboiler inlet, preboiler outlet and test section outlet are measured with W-3%Re vs. W-25%Re bare-wire thermocouples located in wells (Figure 5).

c) Pipe wall temperatures are measured with W-3%Re vs. W-25%Re thermocouples. Figure 8 shows typical thermocouple junctions on the test section wall. The junction is made by resistance welding the 0.005-inch thermocouple wires to the pipe wall. A continuing problem in the 100 KW Facility has been repeated failures of the wall thermocouples. One mode of failure has been due to the W-3%Re leg of the thermocouple lifting off the pipe surface. It was found that a small tab of 0.002-inch thick tantalum foil tacked over the junction reduces the frequency of this type of failure. However, due to the severe operating conditions imposed on the test section, wall thermocouple failures remains one of the chief causes of loop "downtime".

e) System pressures are monitored with two slack-diaphragm type pressure transducers located upstream and downstream of the inlet throttling orifice. The argon pressure in the dump tank is an additional indication of system pressure, since the loop is normally operated with the dump tank valve open.

Test section thermocouples are calibrated in-loop as follows. With the test section mass velocity held constant at a relatively low value, the preboiler power is increased to a level such that the vapor quality of the potassium entering the test section is about 10%. Neglecting the small temperature changes due to pressure drop the temperature of the two-phase fluid in the test section is assumed to be uniform. After the system has reached a steady-state condition, the test section heat loss is determined using the radiation-case temperatures. The test section power is then increased until the electrical power input balances the heat losses. Under these very nearly isothermal, adiabatic conditions, the temperatures of all test section thermocouples closely approximate each other. Using one of the test section outlet well thermocouples as the standard, a thermocouple correction is obtained for each of the test section thermocouples by comparison with this standard thermocouple.

Since an applicable national standard EMF-temperature table has not been adopted, samples from the same spool of W-3%Re vs. W-25%Re thermocouple wire used in the 100 KW Facility are calibrated in a vacuum furnace. Initial calibrations of this kind indicated a drift of about 20°F. However, after the thermocouples were "soaked" for a few hours at 2300°F, repeatability to within ± 3°F was obtained. As part of the procedure for in-loop calibrations, newly installed thermocouples are held at 2100°F for at least five hours before taking the first calibration reading. Two additional calibration readings are then taken at one hour intervals to verify absence of drift.

DATA MEASUREMENT AND REDUCTION

It is useful at this point to define the various regimes of forced convection boiling encountered in the "once-through" boiling tests in the 300 KW Facility and in the tests in the 100 KW Facility, as the experimental techniques depend to some extent on the boiling regime being investigated.

The "nucleate" boiling regime exists in the lower range of vapor qualities extending to some upper quality level which is dependent on the heat flux for a given flow geometry, flow rate and saturation temperature. This regime is characterized by relatively high heat transfer performance (heat transfer coefficients of the order of 10,000 Btu/hr-ft^2-$^\circ$F) and steady or only slightly fluctuating wall temperatures. It is believed that in the nucleate boiling regime the heated wall is entirely wetted by liquid, possibly by a continuous liquid film for forced convection bulk boiling. As heat flux or vapor quality is raised, the nucleate boiling regime is eventually terminated by onset of the "critical heat flux" condition, as characterized by beginning of substantial wall temperature fluctuations and reduction of heat transfer performance. This marks the beginning of the "transition" boiling regime, for which the wall temperature fluctuates markedly and the effective heat transfer coefficient is significantly less than for the nucleate boiling regime (heat transfer coefficients of the order of 1,000 Btu/hr-ft^2-$^\circ$F or less). It is thought that in the transition boiling regime the wall is only intermittently wetted by liquid. Further increases in heat flux and vapor quality result in increased fluctuations of the wall temperature until finally stable "film" boiling occurs, as characterized by relatively steady, but large wall-to-fluid temperature differences and correspondingly poorer heat transfer performance, with heat transfer coefficients comparable to those for dry vapor flow. In the film boiling regime the heated wall is believed to be completely dry with the liquid being carried along as droplets in the stream and with the heated wall in contact with locally superheated vapor.

<u>300 KW Two-Fluid Boiling Tests</u>

Figure 9 shows the measurements made for a typical once-through boiling run to exit superheat conditions in the 300 KW Facility using a helix insert in the test section. Four distinct heat transfer regimes may be inferred, namely: sub-cooled liquid heating, nucleate boiling, transition boiling, and vapor superheating.

The data for this typical run, as shown in Figure 9, do not provide a basis for distinguishing the film boiling regime from the transition boiling regime. It is possible that due to the controlled temperature characteristics of the two-fluid boiler, the corresponding upper limit of the wall-to-fluid temperature difference is not high enough to cause complete drying of the heated wall prior to reaching dry vapor flow conditions, as is required for onset of the film boiling regime.

The discontinuity of slope in the sodium temperature profile indicated by the shell temperature measurements shown in Figure 9 is assumed to be the critical heat flux point and the beginning of transition boiling. The position at which the potassium temperature begins to rise near the tube exit is assumed to mark the beginning of the superheated vapor region. The amount of heat transferred in the superheat region is calculated from the measured potassium temperature rise to the exit. The point of boiling inception and the amount of heat transferred in the subcooled liquid region are similarly determined from the insert thermocouples. For runs in which no insert was used superheated vapor exit conditions were not attained and, consequently, only the subcooled heating region and nucleate and transition boiling regions were present. For these runs without insert, the potassium temperature at boiling inception was obtained using the inlet pressure gage in conjunction with saturation temperature-pressure properties, and the subcooled heating length was determined by single-phase heat transfer calculations.

The average heat flux in the nucleate boiling region is calculated from the axial shell temperature gradient in this region, which is assumed to be equal to the sodium axial bulk temperature gradient. From the average heat flux and the length of the nucleate boiling region, the amount of heat transferred in the region is calculated. The heat transferred in the transition boiling region is determined as the difference between the total heat input and that transferred in the other regions. The average heat flux in the transition region is then calculated from the estimated length of the region.

The local vapor quality and local sodium temperature at various points along the tube, including the critical heat flux point, are calculated by heat balance, employing the values of heat flux and length determined for the various regions. The local potassium temperature, obtained from the insert thermocouples, and the calculated local sodium temperatures are utilized to calculate overall heat transfer coefficients for each of the various regions. From these coefficients a potassium heat transfer coefficient for each region is obtained by subtraction of the thermal resistances of the sodium and boiler tube wall from the respective overall thermal resistances.

The average nucleate boiling heat transfer coefficients calculated in the above manner are large compared to the tube-wall and sodium coefficients and therefore represent a small fraction of the overall thermal resistance in the nucleate boiling region. This fact precludes their accurate determination in the 300 KW Facility; but correspondingly the overall heat transfer coefficient in the nucleate boiling region, which includes the average nucleate boiling heat transfer coefficient and the effective coefficients for the tube wall and the sodium, both of which are known with reasonable accuracy, can be employed to calculate with good accuracy values of the heat flux in that region. In particular, the critical heat flux is calculated as the product of the overall heat transfer coefficient in the nucleate boiling region and the measured sodium-to-potassium temperature difference at the critical heat flux point.

The error in the critical heat flux levels calculated in the above manner is not expected to be large. The potassium nucleate boiling heat transfer coefficient should be largest just upstream of the critical heat flux point since both heat flux and vapor quality increase towards the critical point, and there is evidence from the 100 KW Facility data (treated subsequently) that the nucleate boiling heat transfer coefficient increases with both of these quantities. If, for example, the potassium heat transfer coefficient were taken to be infinite in the calculations, the corresponding critical heat flux level would be increased by less than 20% over that determined by the above procedure.

The error in the local vapor quality, including the quality at inception of critical heat flux conditions, is estimated to be about 5% from a consideration of flow and heat balance errors. As mentioned above, the error in the nucleate boiling coefficient is large since it is a small part of the overall resistance. Since the transition boiling heat transfer coefficients are smaller than the nucleate boiling coefficients, they represent a greater share of the overall thermal resistance and thus can be determined with greater accuracy. The major sources of error in the determination of the transition boiling heat transfer coefficient are the uncertainty of the transition boiling length, because of the limited number of insert and shell thermocouples, and the error in the calculation of the heat transferred in this region. An estimate of the error in the transition boiling heat transfer coefficients is $\pm$ 25%.

100 KW High-Temperature Boiling Tests

The test procedure used in the 100 KW Facility is to hold the saturation temperature, test section mass velocity and test section heat flux nearly constant while the test section vapor quality is varied by changing the preboiler power.

Heat transfer coefficients are calculated from measurements made at a station inside the heated zone about 2-inches upstream of the test section exit. The heat flux, which is assumed uniform over the heated length, is calculated from the measured electrical power input, and is corrected for heat losses. The inside wall temperature is calculated using the measured outside wall temperature and the calculated temperature drop across the pipe wall. The local fluid temperature is measured by the three well thermocouples at the test section exit.

The error in the nucleate boiling heat transfer coefficients is estimated to be within about $\pm$ 45%, due primarily to the small wall-to-fluid temperature differences, which are typically less than about 10°F. For the film boiling and superheated vapor heat transfer coefficients the error is estimated to be within about $\pm$ 10%.

Onset of critical heat flux conditions is detected by observing the behavior of the test section wall temperatures as they are recorded on an 8-channel oscillograph recorder. The behavior of the test section wall temperature at the onset of the critical heat flux condition was found to be of two general types, as follows. At relatively high heat fluxes, when the critical heat flux condition was reached (by slowly increasing test section inlet vapor quality) the wall temperature at the test section exit would suddenly begin to rise on a rapid transient ($\approx 50^{o}$F/sec.) sharply distinguishable from the small wall temperature fluctuations ($\lessapprox 5^{o}$F) typical of nucleate boiling conditions. Presumably, if no corrective action had been taken, the wall temperature would have continued to rise until stable film boiling was established — or some limit to the process occurred such as a test section failure or reduction of heat flux due to increased heat losses caused by the correspondingly higher radiant heater temperatures. Such runs were terminated by either automatic or manual reduction of the test section power after the wall temperature transient had begun, in order to protect the test section from damage.

At relatively low heat fluxes and correspondingly higher exit vapor qualities, onset of the critical heat flux condition is not so definite. Under conditions of low heat flux, when the vapor quality is raised beyond a certain critical value, which is dependent on the heat flux level, there results a corresponding increase is amplitude of wall temperature fluctuations above that characteristic of the nucleate boiling regime, as illustrated in Figure 10. Further increases in vapor quality result in corresponding increases in the amplitude of the wall temperature fluctuations and the time-average wall-to-fluid temperature difference until, at sufficiently high vapor qualities, stable film boiling occurs.

As illustrated in Figure 10, the amplitude of the wall temperature fluctuation increases continuously from nucleate boiling through transition boiling to film boiling as the vapor quality is raised. Thus, the "critical quality" corresponding to the critical heat flux condition cannot be definitely determined. The criterion which has been arbitrarily selected as a working definition for runs in which this type of behavior occurs is that for a given heat flux the "critical quality" is that quality for which the time-average fluctuating wall-to-fluid temperature difference becomes approximately equal to twice the corresponding steady-state nucleate boiling temperature difference. For data taking purposes, the time-average fluctuating wall temperature at the critical heat flux condition is estimated directly from the oscillograph recorder charts made for each of the test runs, and a constant value of 10,000 Btu/hr-ft^2-^{o}F is taken as a representative average of the steady-state nucleate boiling heat transfer coefficient over the range of variables covered by these tests.

For runs in which an estimate of the effective heat transfer coefficient in the transition boiling regime is made, the procedure used is to calculate a time-average wall temperature from digital recorder data, taken at 3-printouts/second for about 1-minute, and to then use this in conjunction with the measured fluid temperature and test section heat flux to calculate a corresponding time-average heat transfer coefficient.

EXPERIMENTAL RESULTS

Pressure Drop Data From 300 KW Facility

The boiling pressure losses in the test section were determined from slack-diaphragm absolute pressure transducers positioned at each end of the boiler tube. Only the pressure losses in test sections with inserts were analyzed, since the pressure losses without inserts were of the same order of magnitude as the accuracy of the gages, about 1 psi. The frictional component of the boiling pressure loss was calculated by subtraction of the momentum pressure loss. The integrated two-phase frictional pressure drop multiplier was computed as the ratio of the two-phase frictional component divided by the pressure drop for all-liquid flowing at the same total flow rate. Using the square root of the liquid to vapor density ratio as an estimate of the slip ratio (Reference 2), the calculated momentum component was generally less than 20% of the total two-phase pressure loss.

The friction factors required for the computation of the liquid potassium pressure drop, necessary for the determination of the two-phase multipliers, were obtained by water pressure drop tests performed on the boiler tubes with inserts. Typical two-phase potassium frictional pressure drop multipliers, calculated from experimental data reported in Reference 5 and 6, are presented in Figure 11. Shown for comparison on Figure 11 are predictions by the "Martinelli" and "Homogeneous" models. These two-phase frictional pressure drop models are derived and discussed in relation to application to potassium flows in Reference 4.

The agreement between theory and experiment shown in Figure 11 is typical of all the pressure drop results obtained with the 300 KW Facility. The experimental values for the potassium two-phase frictional pressure drop multipliers generally fall between the predictions of the two models.

Nucleate Boiling Data

Figure 12 is a plot of a typical set of nucleate boiling heat transfer coefficients measured with a tube without insert in the 100 KW Facility. At constant saturation temperature, mass velocity and heat flux, the heat transfer coefficient is apparently almost independent of vapor quality over the range shown. The data indicate a trend of increased heat transfer coefficient with increased heat flux. These data are reported together with other nucleate boiling data from the 100 KW Facility in Reference 7.

Measured Temperature Behavior at Post-Critical Heat Flux Conditions

Figure 13 is a segment of a typical oscillograph recorder chart obtained during a critical heat flux determination at a heat flux of 211,000 Btu/hr-ft^2 in the 100 KW Facility. Prior to the preboiler power increase (test section inlet quality increase), the pressure downstream of the orifice, the flow rate and the fluid temperature at the test section outlet were steady and the test section wall temperature had small random oscillations, characteristic of nucleate boiling. Following the power increase, the wall temperature began an abrupt, rapid transient which actuated the automatic power reduction system. This run is typical of the type of wall temperature behavior observed when the critical heat flux condition is exceeded at heat fluxes above about 150,000 Btu/hr-ft^2, in tubes without inserts.

Figure 14 shows segments of a continuous oscillograph recorder chart obtained during a run in the 100 KW Facility during which the heat flux was low, about 50,000 Btu/hr-ft^2. The time of day during the run when each segment was taken is marked on the recording in hours. This run illustrates the general behavior of the test section wall temperature as conditions are changed sequentially from the nucleate boiling regime into transition boiling, stable film boiling and finally into superheated vapor conditions. In segment-1, before the preboiler power increase, the test section is apparently in nucleate boiling although there is an occasional small excursion in the wall temperature indicating that the critical heat flux condition was imminent. Immediately following the preboiler power increase (segment-1), the amplitude of the wall temperature oscillations momentarily reached values up to about 50°F and then became more steady. In segment-2, after the next preboiler power increase, the amplitude of the wall temperature oscillations increased markedly to values of about 75°F with a peak value of almost 150°F, indicating that the test section outlet region was in transition boiling. Following a further preboiler power increase, in segment-3, the wall temperature started to rise steadily and finally reached a maximum and leveled off in stable film boiling. In segment-4, the preboiler power was again increased, resulting in slightly superheated vapor at the test section outlet, as indicated by the rise in measured bulk fluid temperature. Further increases in power (segment-5) resulted in a measured outlet vapor superheat of about 200°F. In segments-6 and -7, the preboiler power was reduced in steps to repeat in reverse the sequence of events observed when going up in preboiler power. The wall temperature behavior during the power reductions is very similar to that observed when increasing power. Heat transfer coefficients calculated from the measured wall temperatures, using the procedures described earlier, are noted under segments-2, -3 and -4 on Figure 14 at the times for which they were calculated, for the transition, film boiling and superheated vapor regimes, respectively.

Figure 15 compares the wall temperature behavior for a tube without insert with that obtained for a tube with a helical insert. The upper recorder chart in Figure 15 shows the characteristic sharp temperature rise at onset of critical heat flux conditions, for the tube without insert. The lower recorder chart segments in Figure 15 were taken with a tube containing a helical insert (P/D = 6). For this run the wall temperature began to oscillate slightly at a quality approximately equal to the critical quality in the run with no insert; but there was no sharp temperature excursion, even though the heat flux levels were the same. Further increases in quality, approaching 100%, resulted in increases in amplitude and mean level of the wall temperature fluctuations, characteristic of the transition boiling regime, but did not result in onset of stable film boiling conditions. This suggests that a helical swirl-generator insert prolongs the transition boiling regime to higher quality levels than would be obtained in a tube without insert for the same heat flux.

Critical Heat Flux Data and Correlation

Critical heat flux data for potassium in vertical up-flow in circular tubes with and without helical inserts, obtained in the 100 KW and 300 KW Facilities, are presented in Figure 16. These data were reported in References 5, 6, 7, 8 and tabulated in References 8 and 9. The data are correlated by the following empirical equation*:

$$q_c'' = \frac{(1 + a_R)^{\frac{1}{4}}}{1 + 2\left(\frac{x_c}{1-x_c}\right)}, \quad \frac{10^6 \text{ Btu}}{\text{hr-ft}^2} \qquad (1)$$

The parameter a_R in equation (1) is the radial acceleration of the fluid at the tube wall, in g's, developed by the helical insert, and is calculated using the following equation:

$$a_R = \frac{2}{D_i\, g_o} \left[\frac{x_c\, G_K\, \pi}{(P/D)\, \rho_v \sqrt{\rho_L/\rho_v}} \right]^2 \qquad (2)$$

Equation (2) is derived and discussed in some detail in Reference 8. The exponent on the quantity $(1 + a_R)$ in equation (1) was suggested by results for pool boiling, for which the critical heat flux is proportional to the fourth root of the acceleration

*Symbols are defined in the Nomenclature listed at the end normal to the heated surface (References 12, 13, 14).

The form of equation (1) with respect to the critical quality x_c is arbitrary, and the two constants in the denominator were determined empirically by best fit to the data given in Figure 16. The trend of decreasing critical heat flux with increasing vapor quality shown by the data in Figure 16 and given by equation (1) is in agreement with the trend shown for water under stable conditions (c.f., Reference 15 and 16).

Equation (1) correlates the experimental data within an average deviation of 31%. Deviations of the individual data points from equation (1) were examined with respect to the significance of other parameters, such as mass velocity and saturation temperature. No trends were evident, indicating that the dependence of the critical heat flux on these parameters is less than the data scatter over the range of test conditions covered.

Transition Boiling Data and Correlation

Transition boiling heat transfer coefficients have been obtained for a variety of test section geometries. These data were reported in References 5, 6, 7, 8 and tabulated in References 8 and 9. The data are plotted in Figure 17 in terms of the following empirical equation:

$$\frac{\frac{h_{TB}}{h_v} - 1}{(1 + a_R)^{1/5}} = 2.55(10^5) \left(\frac{1-x}{x}\right)^{0.7} \left(\frac{1}{\Delta t}\right)^2 \qquad (3)$$

Equation (3) was derived using the following reasoning:

1) The results from potassium droplet vaporization experiments by Geoscience (Reference 11) show that the vaporization lifetimes of single droplets increase rapidly with increasing temperature difference between the heated surface and the droplet before the onset of complete film boiling. This suggested that the wall-to-fluid temperature difference Δt is an important parameter affecting the heat transfer coefficient in transition boiling.

2) The local vapor quality x is considered an important variable, because the amount of liquid which can be in contact with the heat transfer surface decreases with increasing quality.

3) The transition boiling heat transfer coefficient h_{TB} should reduce to the vapor phase heat transfer coefficient h_v at 100% quality.

4) The radial acceleration generated by a helical insert a_R, given by equation (2), should increase the transition boiling heat transfer coefficient, because the centrifugal force generated tends to increase the fraction of liquid in contact with the heat transfer surface.

The Colburn equation (Reference 18) was used to calculate the vapor phase heat transfer coefficient h_v in equation (3) for the tubes without insert. For the data taken in tubes with helical inserts h_v is calculated from the following empirical equation, which is developed in Reference 8 using Greene's data for liquid water in helical flow (Reference 19):

$$\frac{h_v D_e}{k_v} = 0.359 \left(\frac{D_e V_H \rho_v}{\mu_v}\right)^{0.563} (N_{Pr_v})^{1/3} \qquad (4)$$

where

$$V_H = V_a \sqrt{1 + \left(\frac{\pi D_i}{P}\right)^2} \qquad (5)$$

and

$$D_e = \frac{D_i \left[1 - \left(\frac{D_{cb}}{D_i}\right)^2\right]}{1 + \frac{D_{cb}}{D_i} + \frac{1}{\pi}\left(1 - \frac{D_{cb}}{D_i}\right)} \qquad (6)$$

All exponents and constants in equation (3) were empirically determined to obtain best fit of the 300 KW Facility transition boiling data. Equation (3) correlates the data from both the 300 KW Facility and the 100 KW Facility, shown in Figure 17, with an average deviation of 24%.

SUMMARY AND CONCLUDING REMARKS

Boiling potassium heat transfer data have been obtained over a range of mass velocities, heat fluxes and qualities at temperatures up to 2100°F in single-tube test sections. These results provide a reasonable basis for thermal design of once-through potassium boilers. The experimental equipment and measurement techniques developed in the course of the work represent an advance in the technology associated with high-temperature boiling of potassium.

Results obtained in the two-fluid 300 KW Facility provide data on local heat transfer performance in the transition boiling and superheated vapor regimes at temperatures up to 1750°F. The results from the radiant-heated 100 KW Facility extend the range of test temperatures up to 2100°F for measurements of local heat transfer coefficients.

The exploratory measurements of critical heat flux conditions and wall temperature behavior in the transition and film boiling and superheated vapor regimes, made in the 100 KW Facility, are useful for application to design and give information on the nature of the forced convection boiling process for potassium at high-temperature and high vapor qualities. It is interesting that the measured wall temperature behavior at onset of critical heat flux conditions and in the transition and film boiling regimes for forced-convection boiling potassium (Figures 13, 14, 15) is similar to the wall temperature characteristics reported for water in forced convection bulk boiling flow (References 15 and 17). This similarity suggests that the underlying physical mechanisms may be nearly the same for the two fluids.

NOMENCLATURE

a_R	Radial acceleration developed by insert, g's
D_{cb}	Diameter of insert centerbody, feet
D_e	Equivalent diameter of boiler tube with insert, feet
D_i	Inside diameter of boiler tube, feet
g_o	Acceleration due to gravity, 32.17 ft/sec^2
G_K	Potassium mass velocity, lb/(ft^2-sec)
h	Heat transfer coefficient, Btu/hr-ft^2-^{o}F
h_{TB}	Heat transfer coefficient in transition region, Btu/hr-ft^2-^{o}F
h_v	Heat transfer coefficient for the vapor, Btu/(hr-ft^2-^{o}F)
k_v	Thermal conductivity of the vapor, Btu/(hr-ft-^{o}F)
N_{Pr}	Prandtl Number, dimensionless
P/D	Twist ratio or pitch-to-diameter ratio, tube diameters for 360^o revolution of insert
q"	Local heat flux, Btu/(hr-ft^2)
q''_c	Critical heat flux, Btu/(hr-ft^2)
T_{sat}	Saturation temperature, ^{o}F
V_a	Axial velocity, feet/sec
V_H	Helical velocity, feet/sec
x	Local quality, dimensionless
x_c	Local quality at point of critical heat flux, dimensionless
μ	Viscosity, lb/(hr-ft)
ρ	Density, lb/ft^3
ρ_L	Liquid density, lb/ft^3
ρ_v	Vapor density, lb/ft^3
$\frac{\Delta P_{TPF}}{\Delta P_o}$	Integrated two-phase frictional pressure drop multiplier, dimensionless
Δt	Wall-to-fluid temperature difference, ^{o}F
ΔT	Temperature difference, ^{o}F
ΔT_{SH}	Bulk superheat of vapor, ^{o}F

LIST OF REFERENCES

1. Affel, R.G., Burger, G.H. and Pearce, C.L., "Calibration and Testing of 2-inch and $3\frac{1}{2}$-inch Magnetic Flowmeters For High Temperature NaK Service", ORNL-2793, March 4, 1960.

2. "Alkali Metal Boiling and Condensing Investigations", Quarterly Progress Report No. 6, Contract NAS 3-2528, SPPS-MSD, General Electric Company, NASA-CR-54037, April 20, 1964.

3. "Alkali Metal Boiling and Condensing Investigations", Quarterly Progress Report No. 7, Contract NAS 3-2528, SPPS-MSD, General Electric Company, NASA-CR-54038, April 20, 1964.

4. "Alkali Metal Boiling and Condensing Investigations", Quarterly Progress Report No. 8, Contract NAS 3-2528, SPPS-MSD, General Electric Company, NASA-CR-54138, October 20, 1964.

5. "Alkali Metal Boiling and Condensing Investigations", Quarterly Progress Report No. 9, Contract NAS 3-2528, SPPS-MSD, General Electric Company, NASA-CR-54215, October 20, 1964.

6. "Alkali Metal Boiling and Condensing Investigations", Quarterly Progress Report No. 10, Contract NAS 3-2528, SPPS-MSD, General Electric Company, NASA-CR-54308, January 20, 1965.

7. "Alkali Metal Boiling and Condensing Investigations", Quarterly Progress Report No. 11, Contract NAS 3-2528, SPPS-MSD, General Electric Company, NASA-CR-54405, April 23, 1965.

8. "Alkali Metal Boiling and Condensing Investigations", Quarterly Progress Report No. 12, Contract NAS 3-2528, SPPS-MSD, General Electric Company, NASA-CR-54739, July 23, 1965.

9. "Alkali Metal Boiling and Condensing Investigations", Quarterly Progress Report No. 13, Contract NAS 3-2528, SPPS-MSD, General Electric Company, October 1965(to be issued).

10. Wesling, G.C., and McCarthy, M.E., "Thermodynamic Properties of Potassium Vapor from $1300^{o}R$ - $2700^{o}R$ - Using Naval Research Laboratory Experimental Data", GE Report R64SD3012, SPPS-MSD, General Electric Company, October 6, 1964.

LIST OF REFERENCES (CONT'D)

11. Poppendiek, H.F., et al., Quarterly Technical Report on High Acceleration Field Heat Transfer for Auxiliary Space Nuclear Power Systems, AEC Contract No. AT(04-3)-409, September 1 to November 30, 1964.

12. Zuber, N., "Stability of Boiling Heat Transfer", Trans. ASME April 1964.

13. Costello, C.P. and Adams, J.M., Paper No. 30, "1961 International Heat Transfer Conference", Boulder, Colorado, August 1961.

14. Usiskin, C.M. and Siegel, R., Trans. ASME, J. Ht. Trans., 83-C pp. 243-253, August 1961.

15. Janssen, E. and Kervinen , J.A., "Burnout Condition for Single Rod in Annular Geometry, Water at 600 to 1400 psia", GEAP-3899, February 1963 (OTS)

16. Tippets, F.E., "Analysis of the Critical Heat Flux Condition In High-Pressure Boiling Water Flows", Trans. ASME, J. Ht. Trans. 86-C pp. 23-33, February 1964.

17. Hench, J.E., "Transition and Film Boiling Data at 600, 1000 and 1400 psi In Forced Convection Heat Transfer To Water", GEAP-4492, February 1964 (OTS)

18. Rohsenow, W.M. and Choi, H.Y., "Heat, Mass and Momentum Transfer", Prentice-Hall, 1961.

19. Gambill, W.R. and Bundy, R.D., "An Evaluation of The Present Status of Swirl-Flow Heat Transfer", ORNL Report (central files number 61-4-61), April 1961.

LIST OF FIGURES

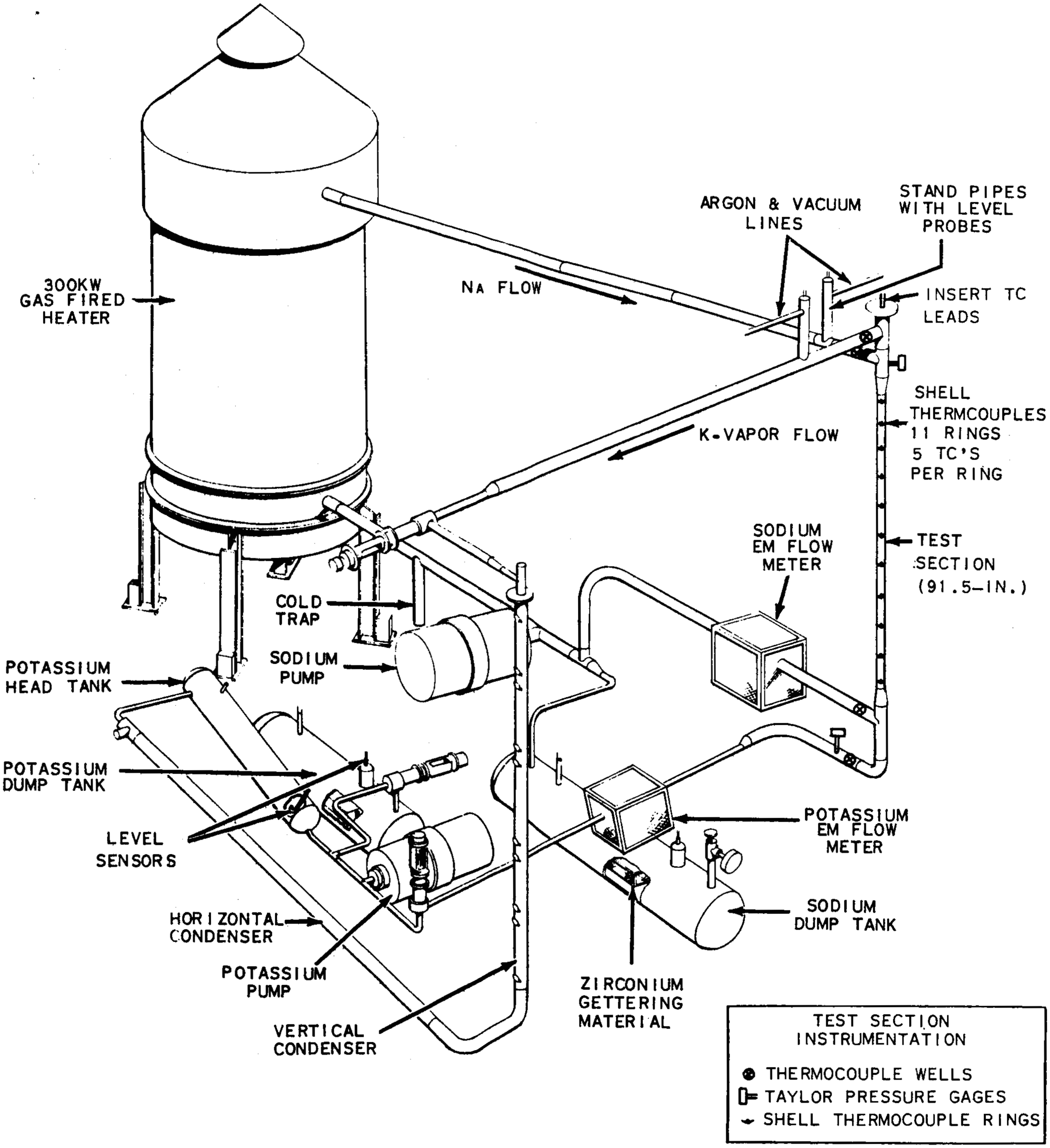

Figure 1 **300KW TWO-FLUID HEAT TRANSFER FACILITY**

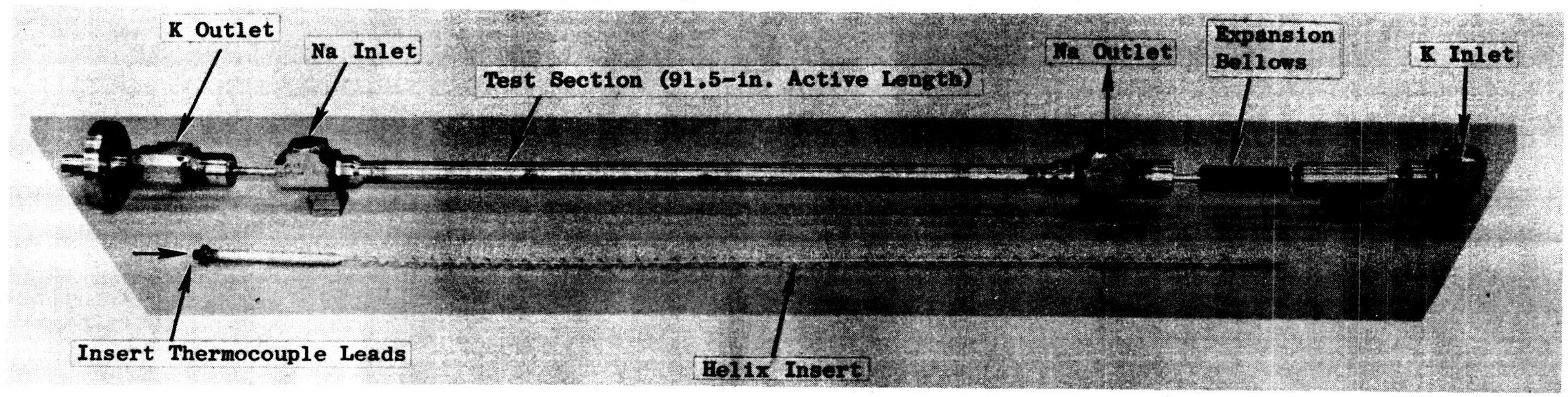

Figure 2 300 KW Test Section With Instrumented Helix Insert

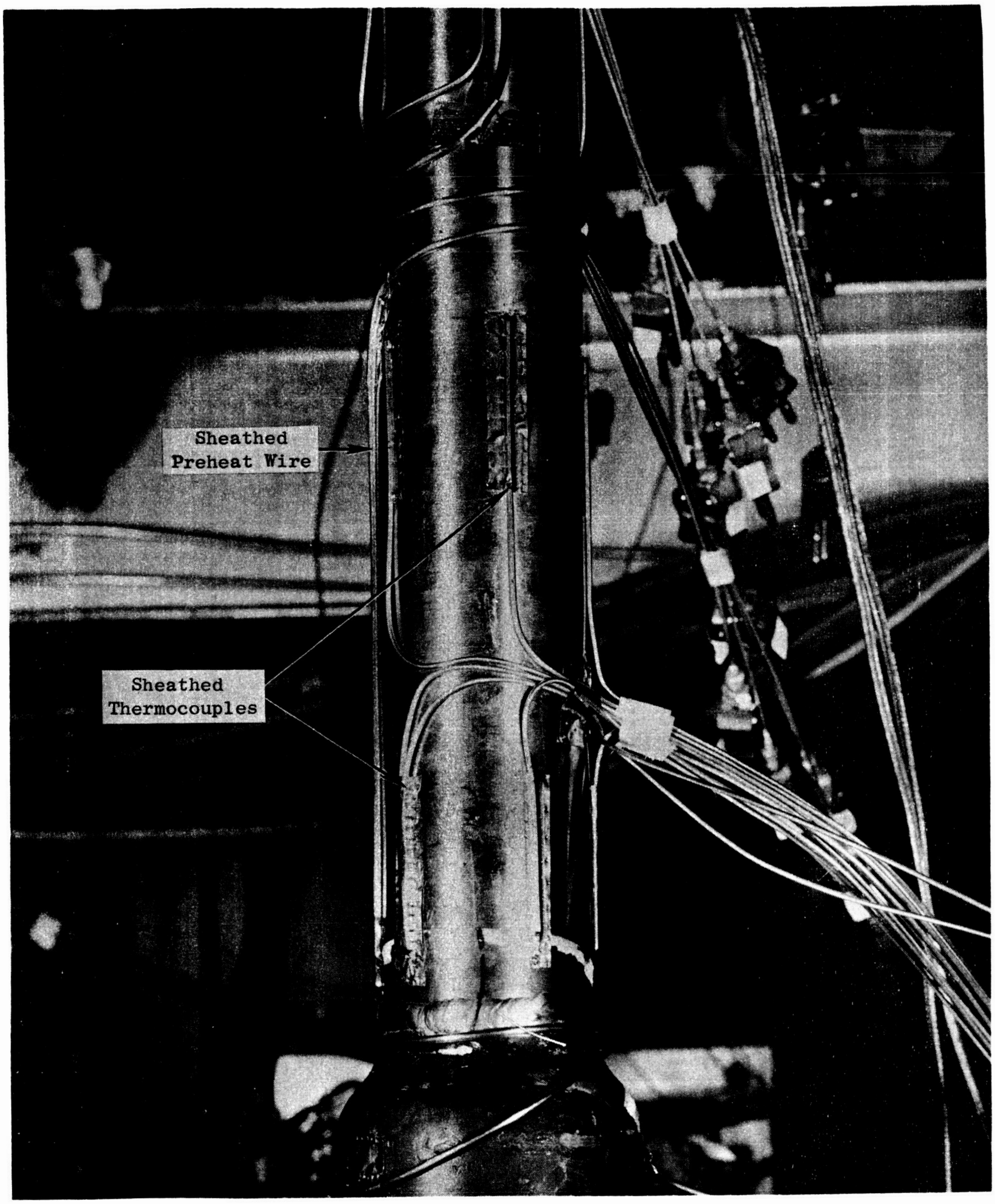

Figure 3 Shell Thermocouple Attachment on 300 KW Test Section

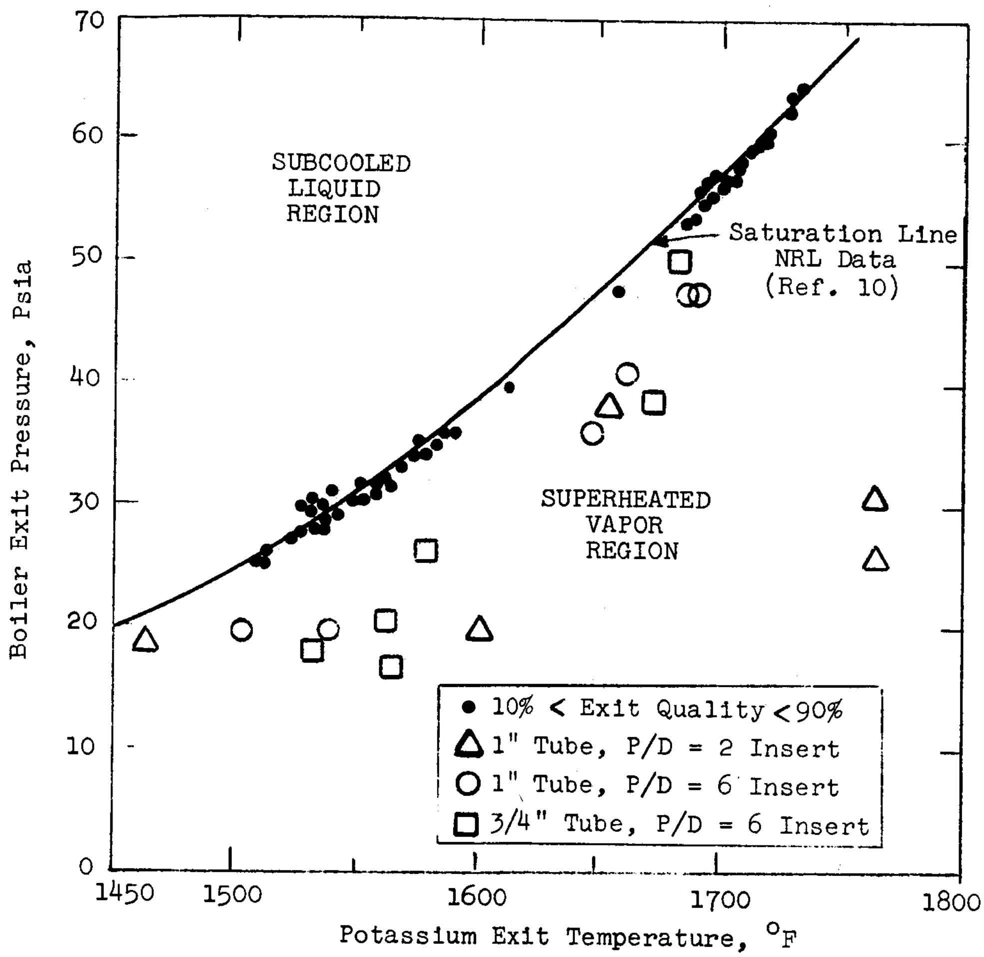

Figure 4. Comparison of Saturation Properties With Measured Potassium Pressures and Temperatures in 300 KW Facility

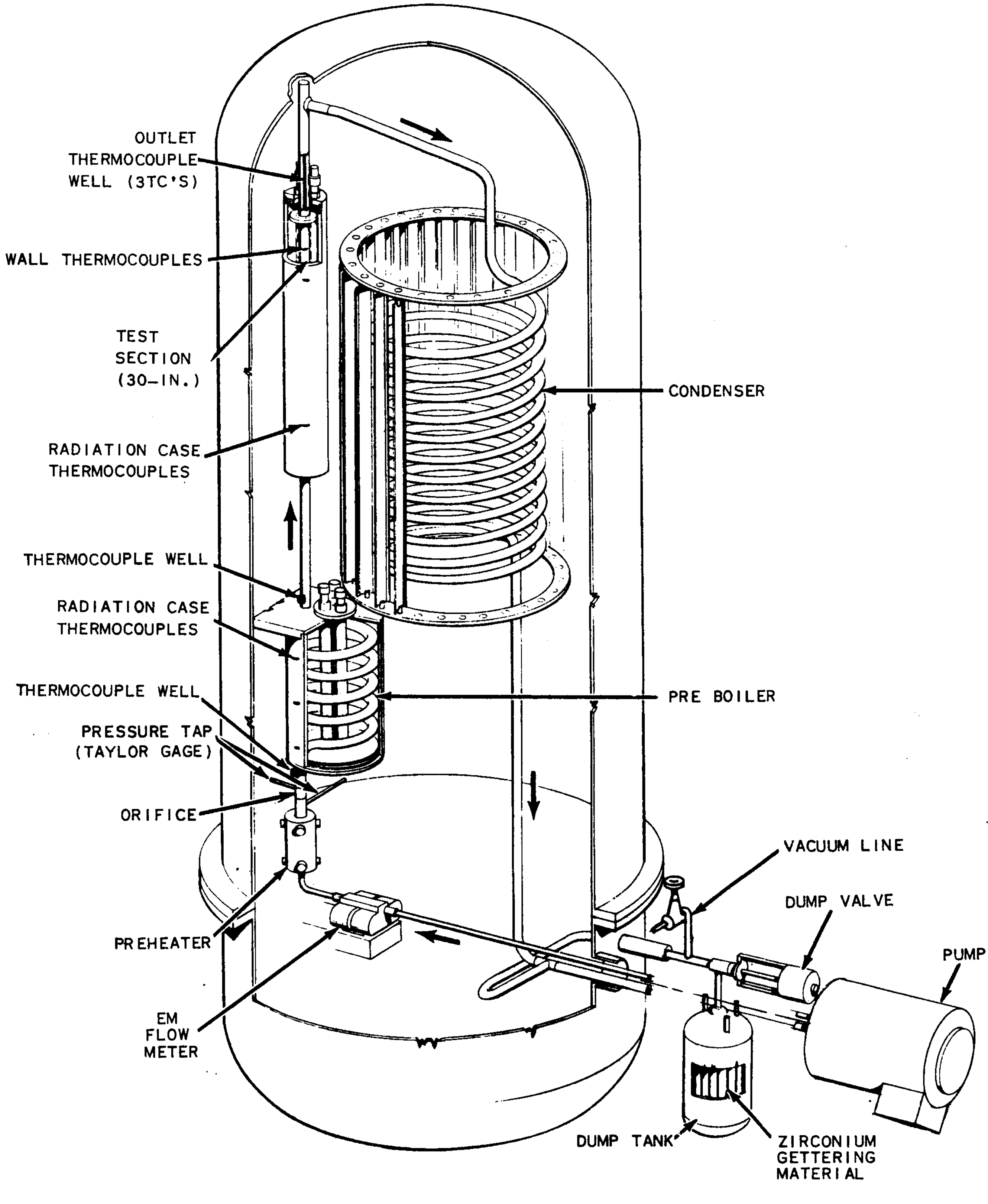

Figure 5 **100KW HIGH-TEMPERATURE HEAT TRANSFER FACILITY**

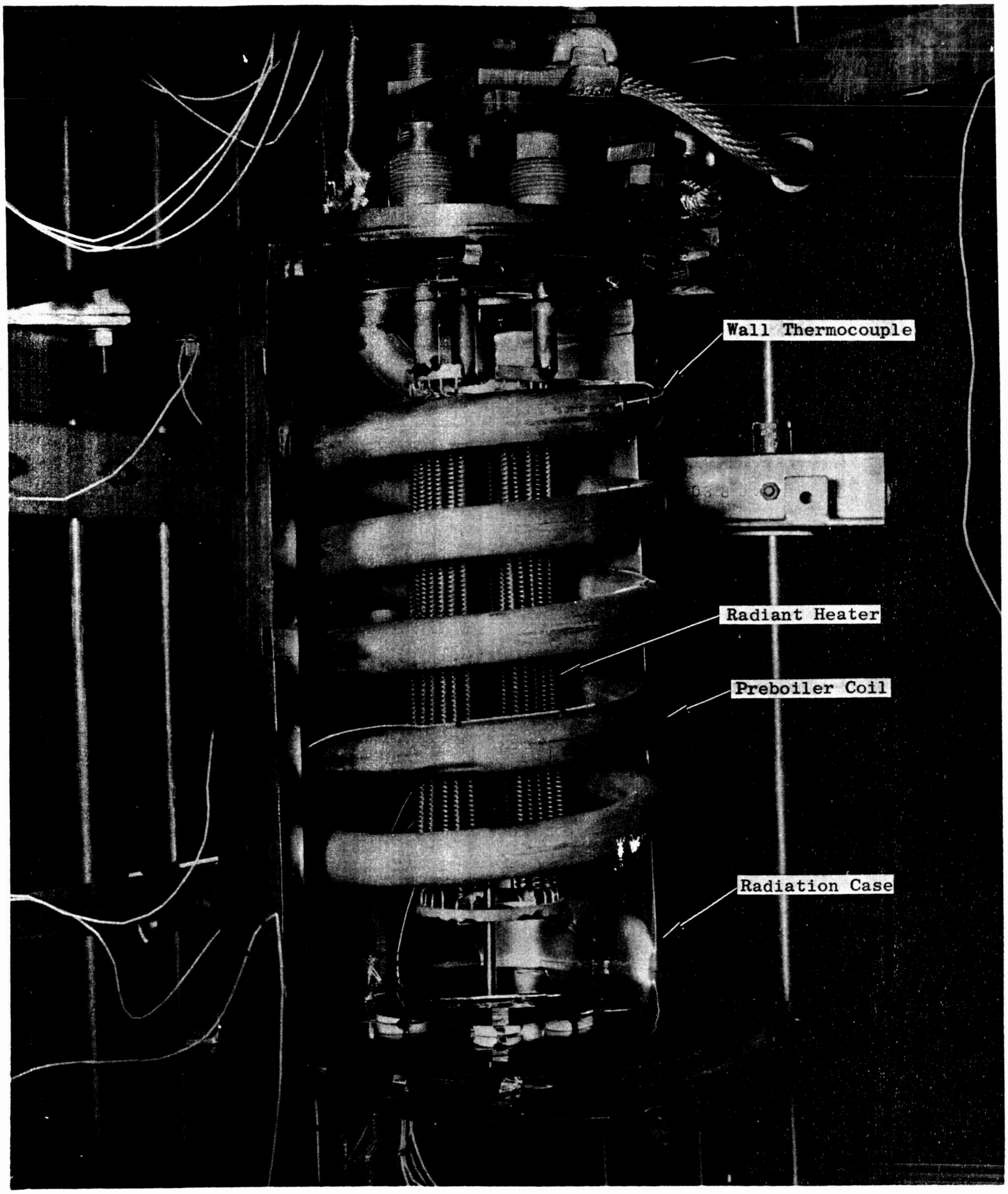

Figure 6 Preboiler for 100 KW Facility

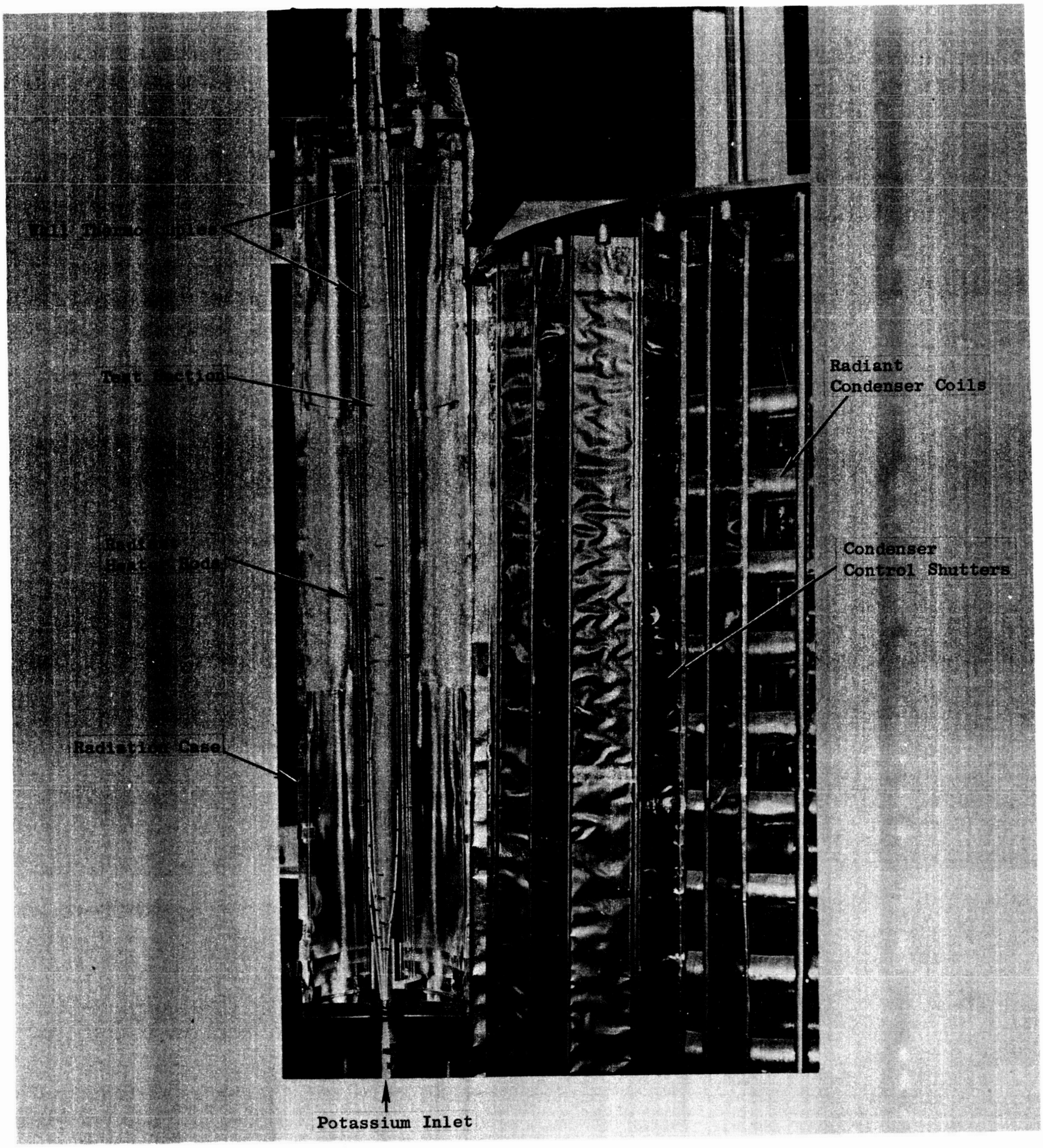

Figure 7 100 KW Test Section Arrangement

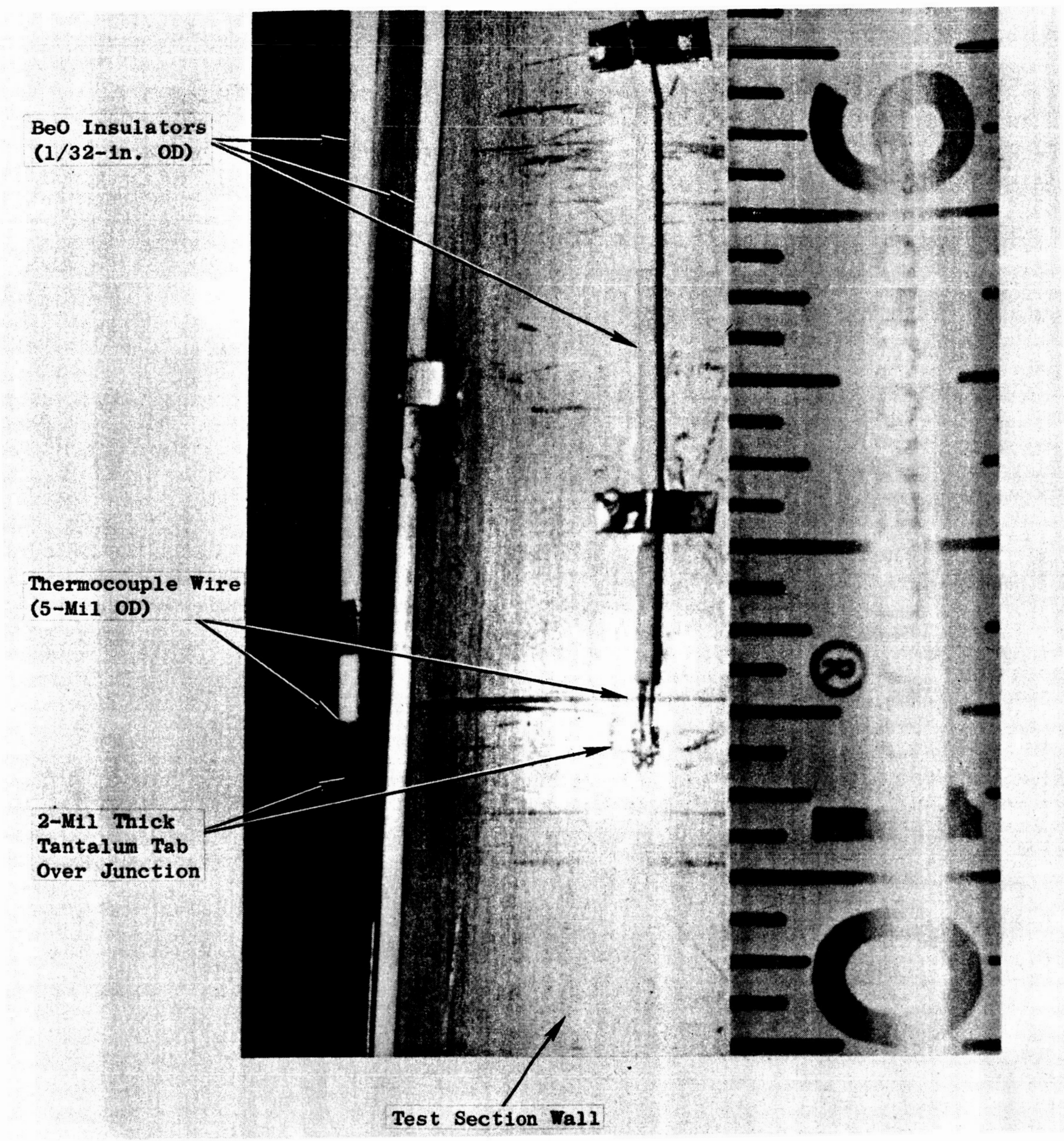

Figure 8 Wall Thermocouple Attachment on 100 KW Test Section

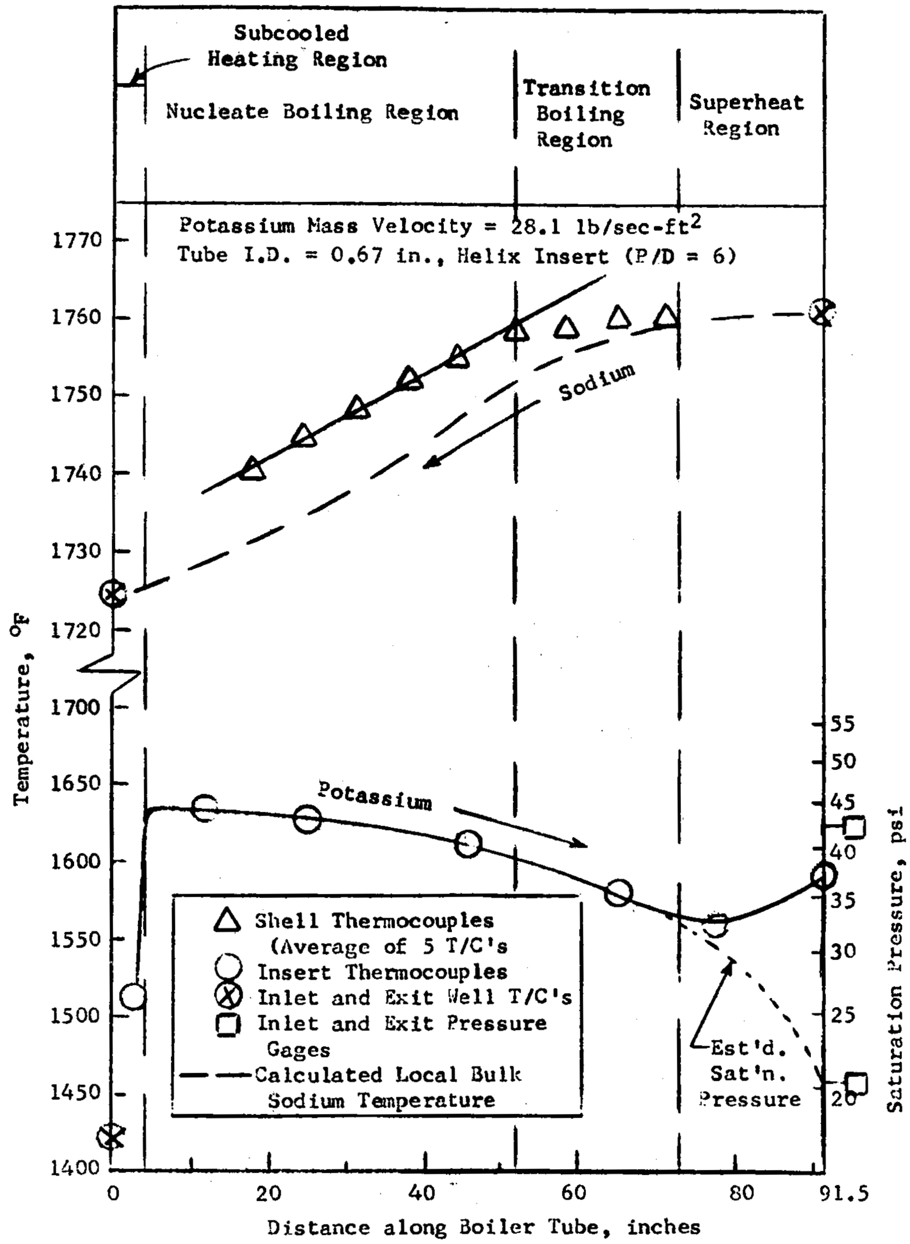

Figure 9. Measured Fluid Temperature Profiles in 300 KW Test Section

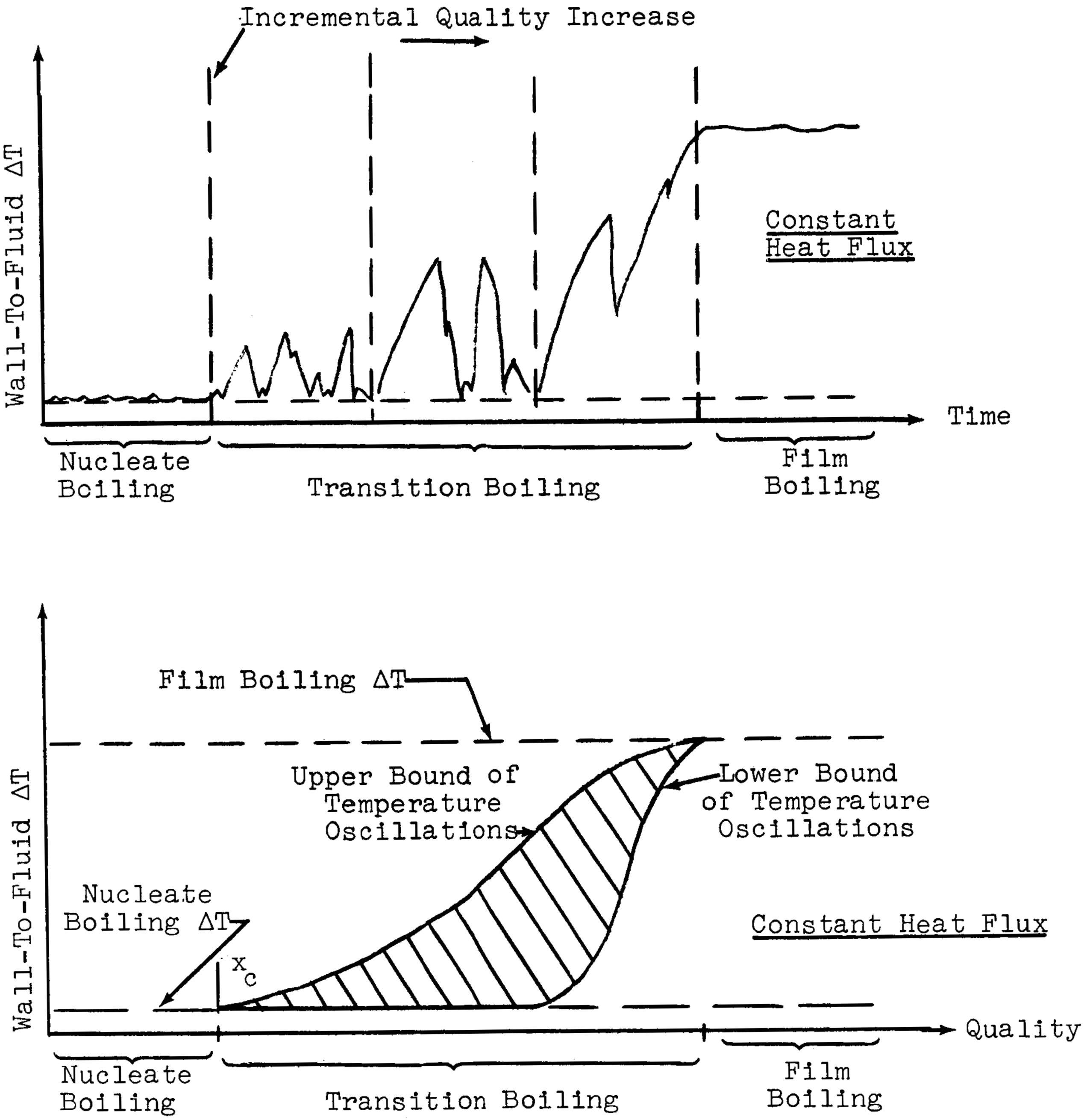

Figure 10 Sketch of Wall Temperature Behavior In Nucleate, Transition and Film Boiling Regimes

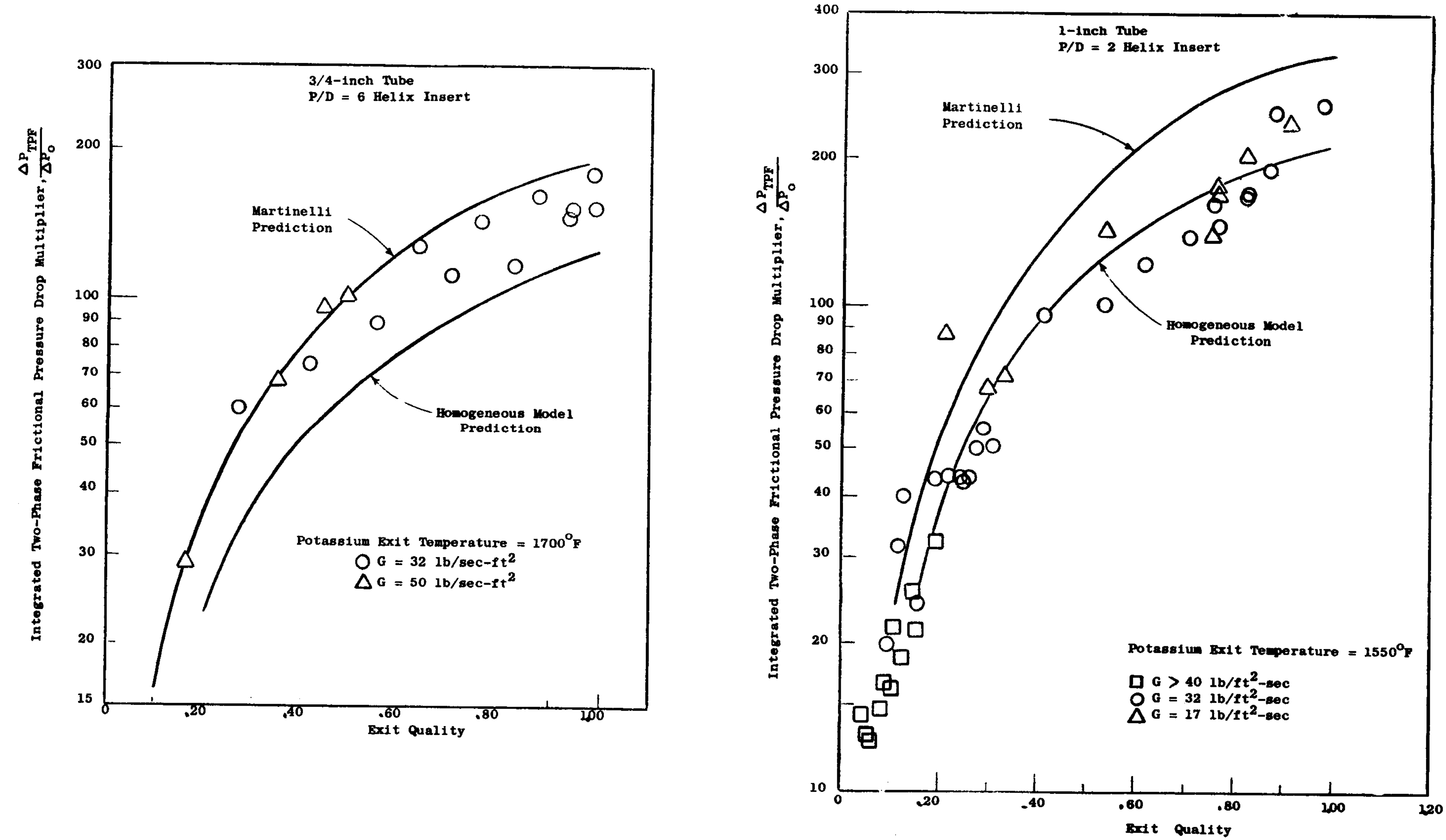

Figure 11. Boiling Potassium Pressure Drop Data From 300 KW Facility

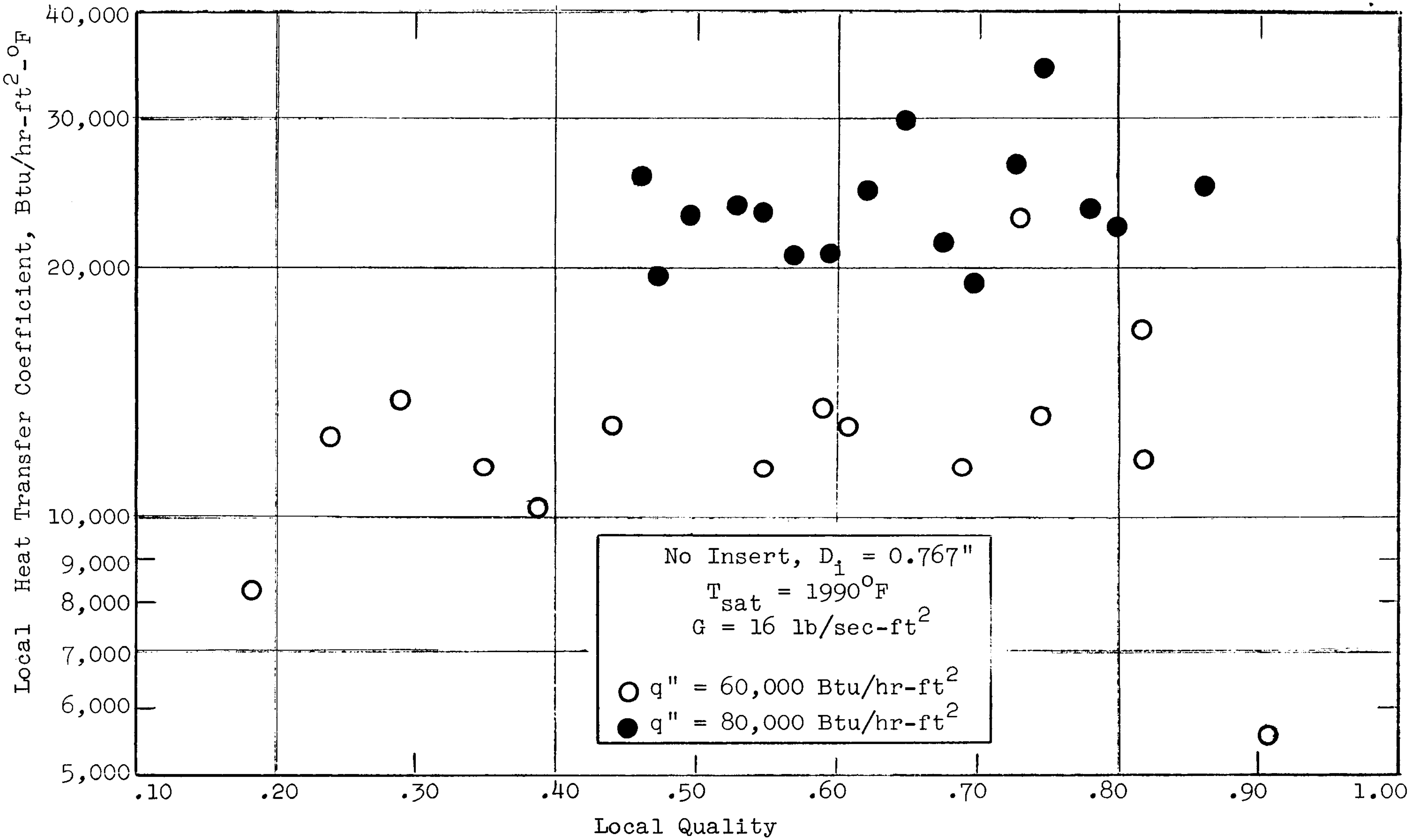

Figure 12. Potassium Nucleate Boiling Data From 100 KW Facility

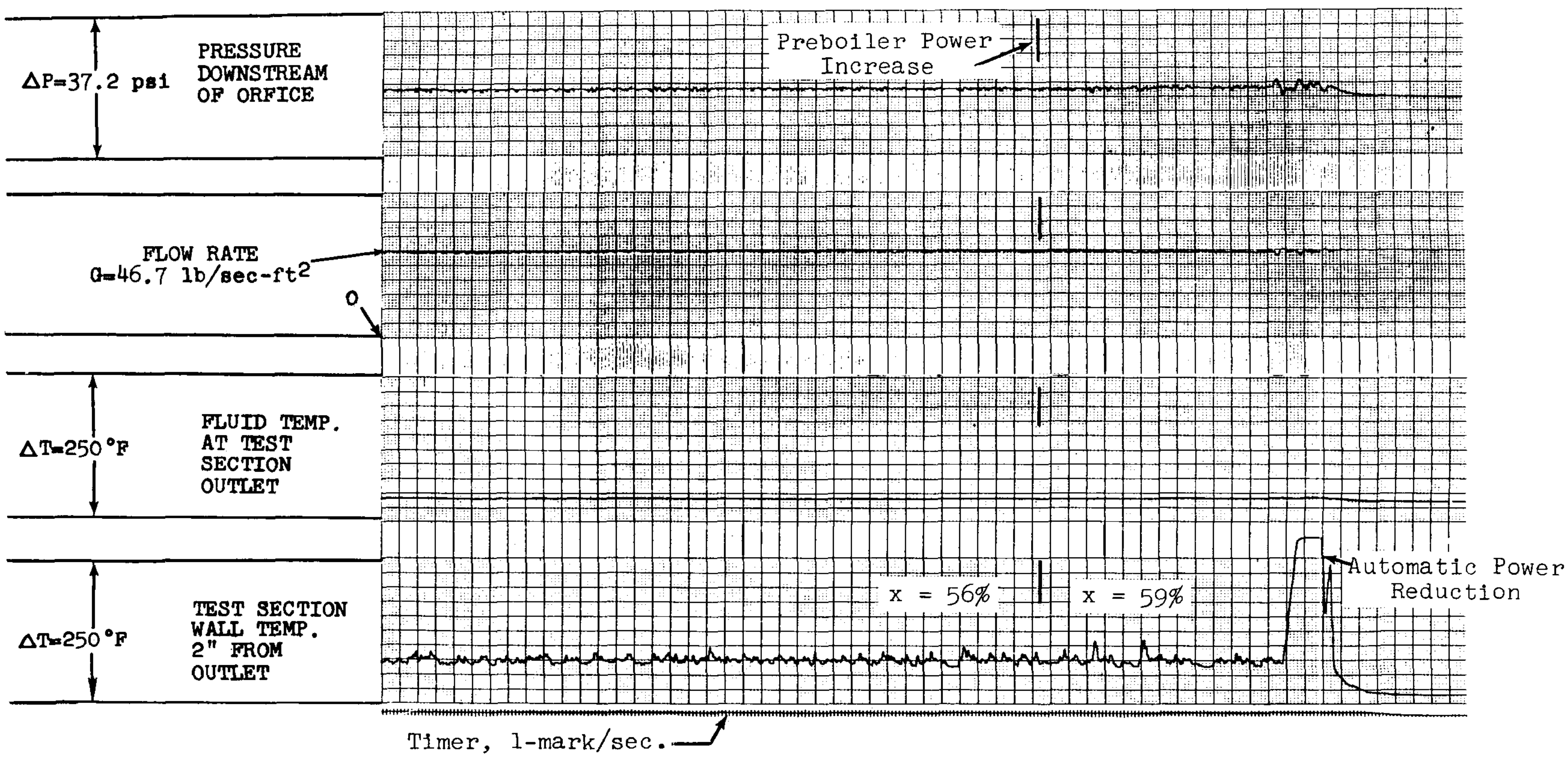

Data taken 4/1/65

T_{sat} = 2105°F
G = 46.7 lb/sec-ft^2
q''_c = 211,000 Btu/hr-ft^2
Test Section ID = 0.423-in. (no insert)

Figure 13 Critical Heat Flux Determination At Relatively High Heat Flux In 100 KW Facility

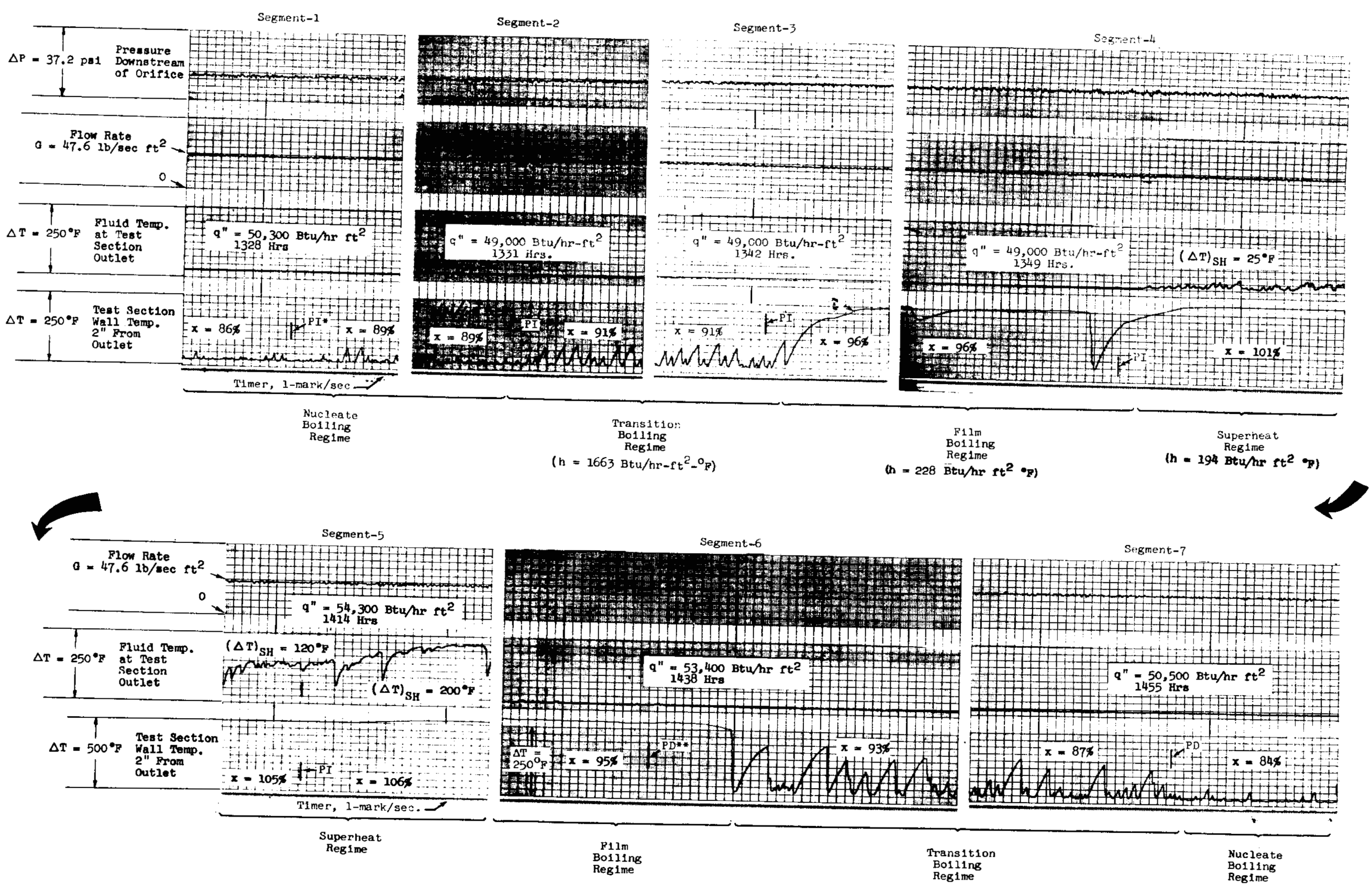

* PI: Preboiler power increase (<5%)

** PD: Preboiler power decrease (<5%)

Test Section ID = 0.423 in.

No insert

T_{sat} = 2105°F

G = 47.6 lb/sec-ft²

Data taken 3/31/65

Figure 14 Wall Temperature Behavior During Operation From Nucleate Boiling to Superheated Vapor Conditions At Low Heat Flux In 100 KW Facility

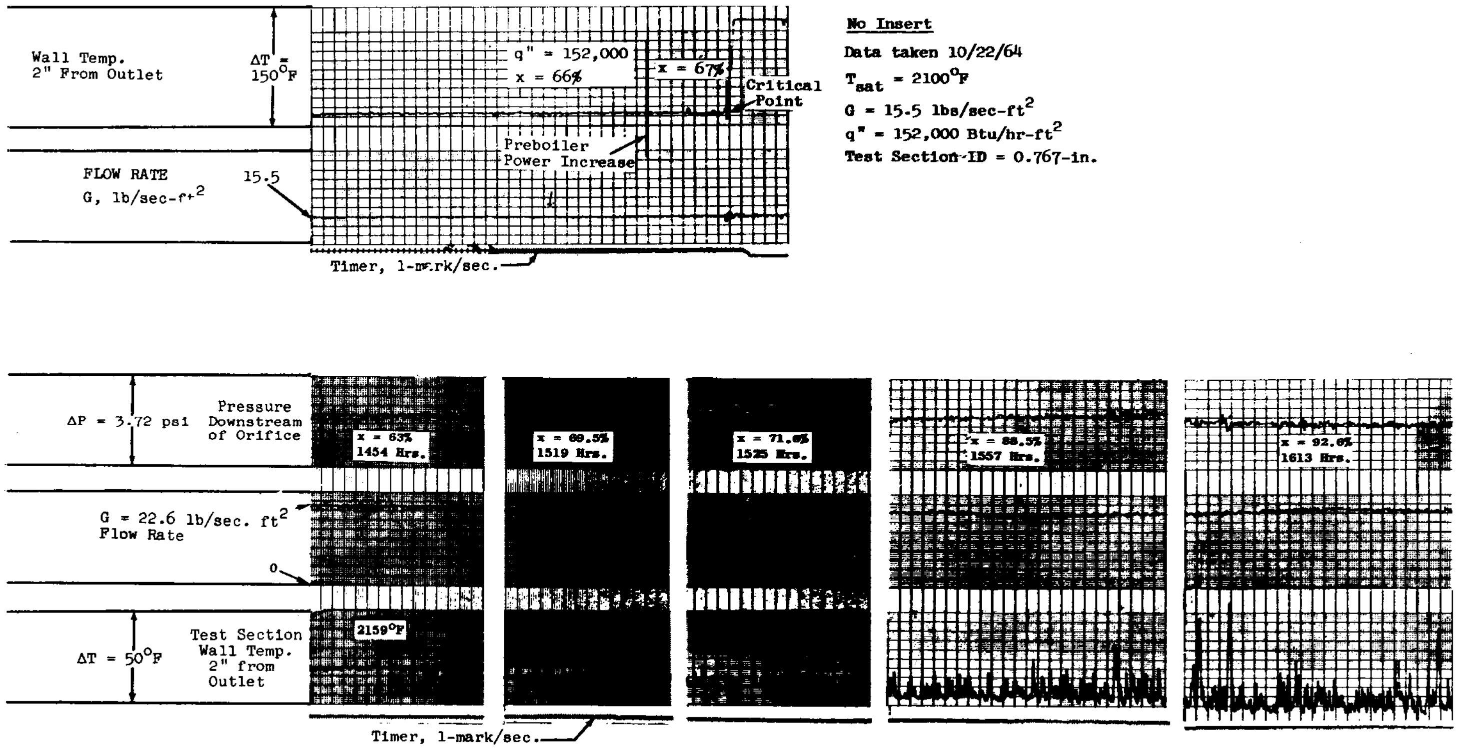

No Insert

Data taken 10/22/64

T_{sat} = 2100°F

G = 15.5 lbs/sec-ft^2

q" = 152,000 Btu/hr-ft^2

Test Section ID = 0.767-in.

Helix Insert (P/D = 6)

Data taken 1/29/65

T_{sat} = 2100°F

G = 22 lbs/sec-ft^2

q" = 150,000 Btu/hr-ft^2

Test Section ID = 0.740-in.

Figure 15 **Comparison of Wall Temperature Behavior At Critical Heat Flux and Transition Boiling Conditions With and Without Helix Insert - In 100 KW Facility**

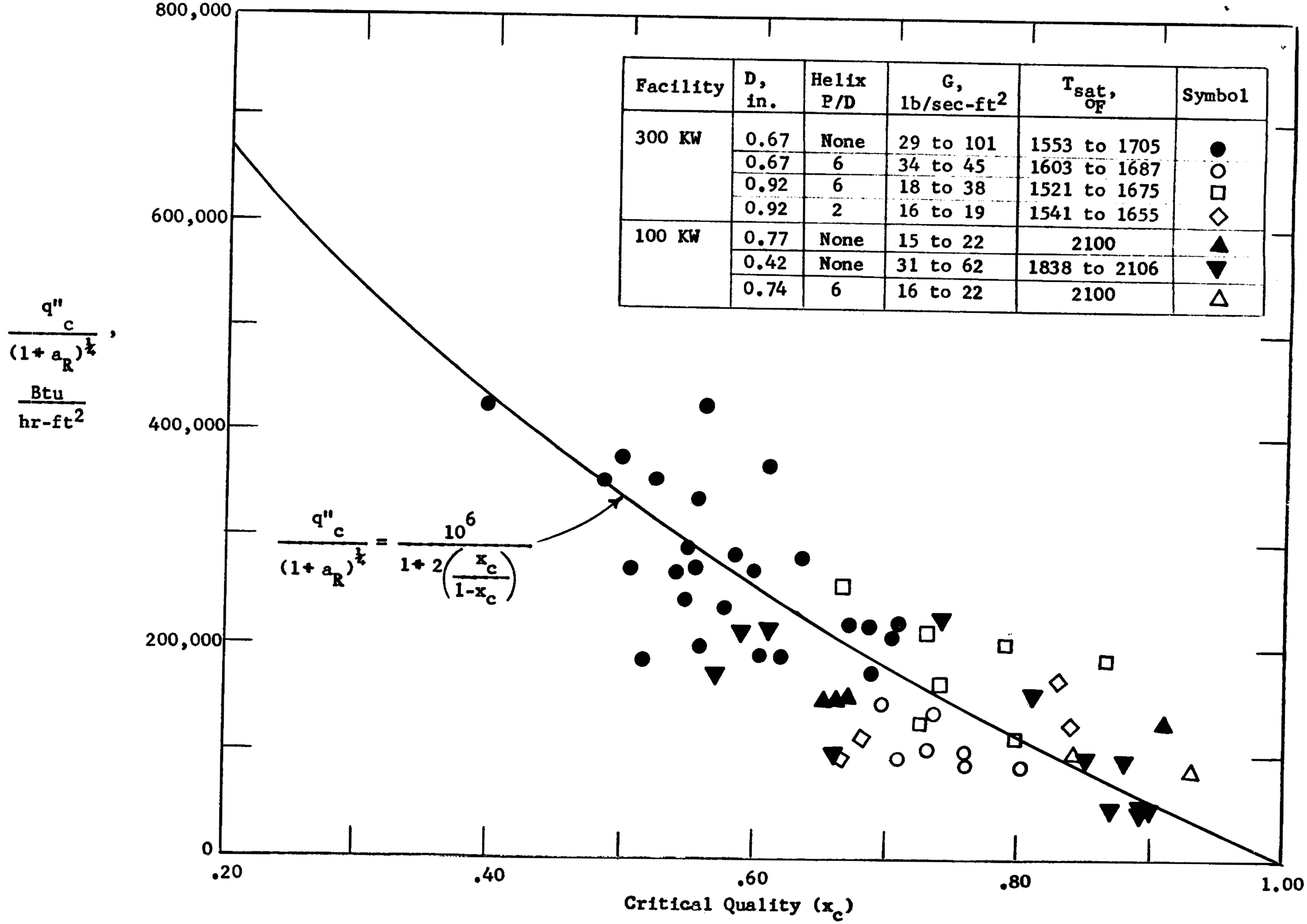

Facility	D, in.	Helix P/D	G, lb/sec-ft^2	T_{sat}, °F	Symbol
300 KW	0.67	None	29 to 101	1553 to 1705	●
	0.67	6	34 to 45	1603 to 1687	○
	0.92	6	18 to 38	1521 to 1675	□
	0.92	2	16 to 19	1541 to 1655	◇
100 KW	0.77	None	15 to 22	2100	▲
	0.42	None	31 to 62	1838 to 2106	▼
	0.74	6	16 to 22	2100	△

Figure 16. Potassium Critical Heat Flux Data and Correlation

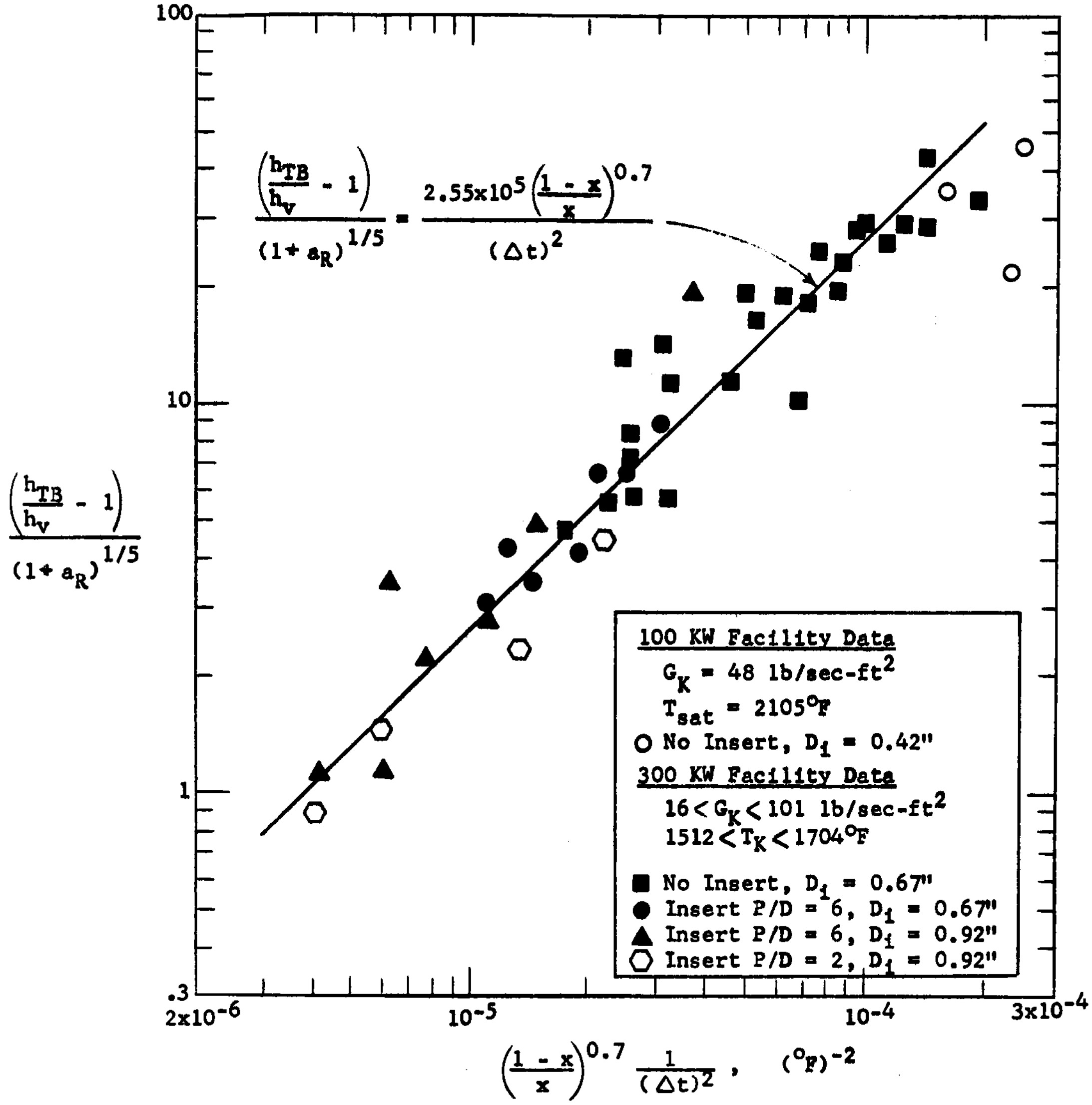

Figure 17. Potassium Transition Boiling Data and Correlation